Available online at www.sciencedirect.com

ScienceDirect

journal homepage: http://www.elsevier.com/locate/acme

Original Research Article

Experimental and numerical two- and three-dimensional investigation of porosity morphology of the sintered metallic material

Lukasz Madej [a,*], Adam Legwand [a], Mateusz Mojzeszko [a], Jacek Chraponski [b], Stanislaw Roskosz [b], Jan Cwajna [b]

[a] AGH University of Science and Technology, Mickiewicza 30 av., 30-059 Krakow, Poland[1]
[b] Silesian University of Technology, Krasinskiego 8 st., 40-019 Katowice, Poland[2]

ARTICLE INFO

Article history:
Received 24 March 2018
Accepted 16 June 2018
Available online 29 July 2018

Keywords:
Numerical modelling
Reconstruction
Computed tomography
Porous material

ABSTRACT

A through scale investigation of a porosity shape and morphology after sintering of the Distalloy AB powder is the goal of the paper. First, the classical two dimensional analysis of porosity geometrical aspects is presented with the use of the systematic scanning technique (SST) and the light microscopy (LM). Then, a three dimensional investigation is realized with the non-destructive computed tomography (CT) technique. Advantages and limitations of the approach are evaluated within the work. Finally, to investigate small pores which are beyond the computed tomography resolution, the destructive serial sectioning technique was applied. The developed three dimensional reconstruction algorithm of two dimensional images of obtained cross sections is also presented. Finally, an example of possible practical application of obtained three dimensional digital representation of porosity in sintered samples, during the finite element (FE) modelling of deformation conditions is presented.

1. Introduction

Sintered porous materials become increasingly popular in various practical applications e.g. in automotive and aerospace areas, because they provide desired physical and chemical properties of products. They also give an opportunity to obtain components with a specific microstructure, porosity and permeability [1]. However, to properly evaluate how porosity influences metals behaviour under processing and exploitation conditions it is crucial to investigate their morphology, size, shape and distribution within the matrix material [2,3]. These are also crucial inputs for a numerical modelling-aided process design as presence of porosity significantly affects three dimensional stress state during deformation leading to local heterogeneities associated with

* *Corresponding author.*
E-mail address: lmadej@agh.edu.pl (L. Madej).
[1] www.msm.agh.edu.pl.
[2] www.inom.polsl.pl.
https://doi.org/10.1016/j.acme.2018.06.007
1644-9665/

e.g. strain localization and fracture [4]. Similar issues have to be faced in many modern multiphase materials.

To capture these heterogeneities, advanced numerical models that take into account 2D or 3D morphology of investigated materials have to be created [5,6]. Such concept is often referred as the Representative Volume Element [7] or the Digital Material Representation (DMR) approach [8].

There are two main approaches for generation of 2D and 3D digital representations of single and multiphase microstructures:

- the first is based on image analysis of metallographic data obtained from light [9] or electron microscopy [10] providing exact representation of microstructure features. That way even highly complex multiphase materials can be easily recreated in a digital form where each microstructural feature is characterized by a unique identifier. The approach is usually used to recreate 2D microstructures due to availability of metallographic data. Development of the 3D digital model requires more sophisticated techniques based on the 3D tomography data (e.g. near-field high-energy X-ray diffraction microscopy or X-ray diffraction contrast tomography) or the serial sectioning approach. X-ray tomography methods are particularly interesting as they are classified as non-destructive approaches giving an opportunity to analyse the same sample region before and after deformation.
- the second is based on numerical methods providing similar representation of microstructure features in a statistical sense. Such synthetic microstructures can be generated both in 2D and 3D computational domains with the use of simplified grain growth [11] or physically based microstructure evolution models [12]. Different numerical methods can be then used for implementation of mentioned models e.g. cellular automata, Monte Carlo, phase field or Voronoi tessellation. However, development of such synthetic microstructure generation algorithms is usually associated with the support of series of above mentioned experimental investigations providing sufficient amount of data for a statistical evaluation of material features. When the algorithm is properly validated it can be used for fast generation of wide range of microstructural features during further numerical investigation of its behaviour under processing conditions.

As presented, both groups of approaches for generation of 3D DMR are usually based on a combination of numerical and experimental investigations, which complement each other. Thus, within the paper, an experimental and numerical investigation in 2D and 3D spaces is carried out with various techniques providing comprehensive information on the porosity morphology in sintered metallic samples across different length scales. Particular emphasis is put on evaluation of advantages and limitations of these approaches in generation of digital microstructure models.

Obtained information can be then directly used as an input for the Digital Material Representation based numerical modelling or can provide data for development of numerical algorithms for a synthetic microstructure generation. Such DMR based modelling can minimize the amount of experimental research and broaden its scope at the same time.

2. A classical two-dimensional investigation

As mentioned, the sintered sample was selected for the present investigation. It is a good representative of materials with highly complex microstructures, with porosity size ranging across different length scales.

Investigated samples with cylindrical shapes φ 12.7 mm $\times$ 15.7 mm have been sintered from the Distalloy AB powder manufactured by the Höganäs company. The Distalloy AB is an iron powder with the following chemical composition: 1.75% Ni, 1.5% Cu and 0.5% Mo. The sintering procedure, in particular, the pressure and the temperature were adjusted in order to obtain a 25% porosity level. This level has been verified by the hydrostatic weighting procedure performed according to the DIN 30911-3.

A classical investigation of porous materials is based on an extensive 2D imaging of the sample cross section as presented in Fig. 1.

The sample was cut using a wire-cutting electrical discharge machine and its surface was prepared for the metallographic investigation by means of vibro-polishing with 0.05 μm suspension of Al_2O_3. The polishing time was set to 30 min to obtain good quality surface and remove any surface heterogeneities introduced by preparation stages.

A light microscopy imaging in the bright field was performed with the Olympus GX-71, equipped with digital camera for high resolution image acquisition. Examples of microstructure images of unetched and etched in 3% nital specimens obtained from the LM are presented in Fig. 2.

A randomly distributed porosity within the uniform matrix is clearly visible in the unetched sample (Fig. 2a). Uniaxial ferrite grains can be additionally revealed after etching as seen in Fig. 2b. Porosity is represented in dark grey colours, which are easily distinguishable from bright ferrite grains. This characteristic provides a possibility to apply image processing techniques for binarization purposes, in order to distinguish the shape of pores in a 2D space. Image analysis was performed with the MetIlo software [13]. In the further examination only images of unetched specimens were used

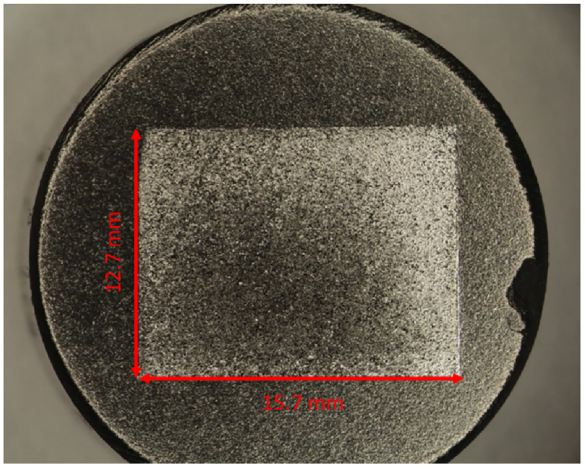

Fig. 1 – A cross section of the investigated cylindrical sample after a sintering process.

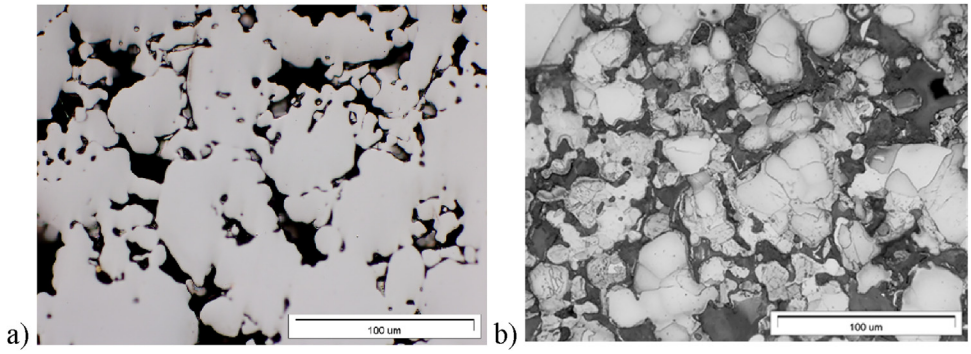

Fig. 2 – Light microscopy images of the investigated samples: (a) unetched specimen and (b) specimen etched in 3% nital.

to avoid any over etching issues, which may affect determination of the porosity fraction. After initial image corrections involving contrast and sharpness adjustments, the binarization with a simple thresholding algorithm was realized. Approach provides a possibility to obtain a binary image on the basis of a properly selected threshold value. Each pixel in the image from Fig. 2 has a specific value of the grey scale and during the thresholding algorithm execution, all pixels with grey scale values below the threshold, are classified as ferrite grains (white colour) and pixels with values higher than the threshold are considered to represent porosity (red colour). After this stage, usually some small image disruptions in the form of the noise or speckles are still visible. To eliminate these disruptions and clearly distinguish between two types of features (matrix and porosity) the filtering algorithm was applied. Additionally, to remove features smaller than 7 pixels a despeckle algorithm was introduced into the procedure. As a result, the binary representation of the investigated region was obtained as seen in Fig. 3.

During the investigation, to accurately evaluate geometrical aspects of porosity (e.g. size, shape, dispersion, etc.) the systematic scanning method [14,15] was used. Series of high resolution images from the entire sample surface were acquired according to the setup presented in Fig. 4. Each image (Fig. 5) was subjected to the same image processing operation as discussed above.

Based on the acquired high resolution images, a quantitative analysis of porosity was performed to evaluate variations in the volume fraction of pores and it was confirmed that the average porosity is 25.21%.

However, if a more detailed investigation is required e.g. regarding geometrical aspects of porosity, the 2D analysis can be misleading, especially if only limited amount of 2D images was provided for the investigation. Images acquired with the scanning electron microscopy and the secondary electrons detector (Fig. 6) have a large depth of focus and reveal that the shape of porosity can be highly complex and irregular along the third dimension, what cannot be properly assessed by 2D images.

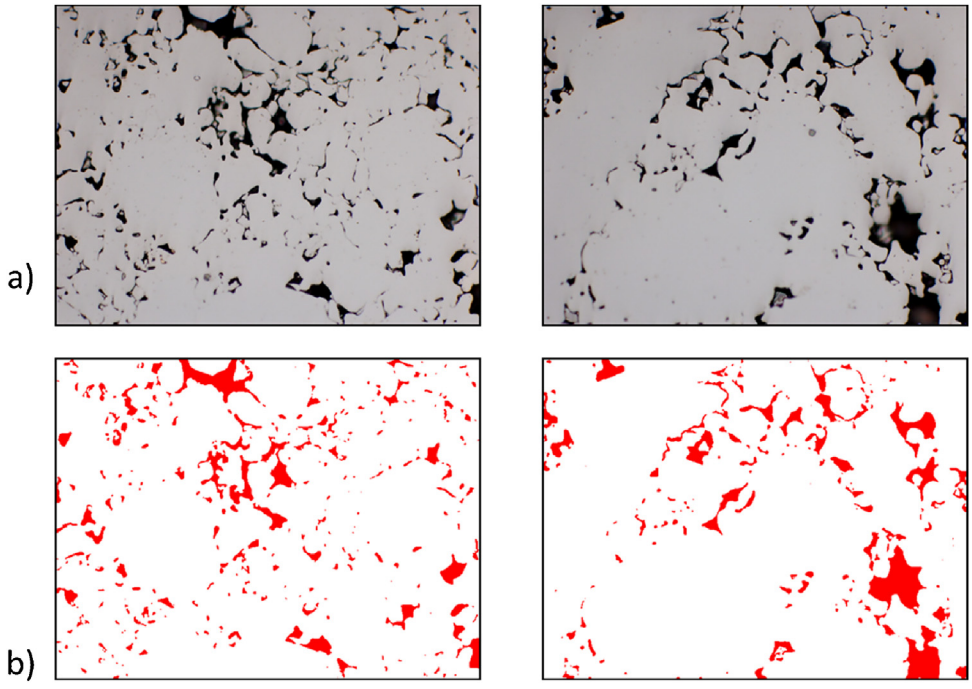

Fig. 3 – Examples of two investigated (a) microstructures and (b) corresponding binary representations.

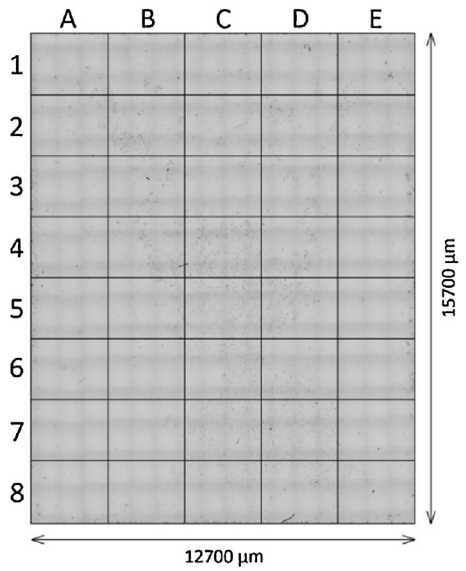

Fig. 4 – Setup of images acquired during the systematic scanning procedure.

Thus, to extend evaluation of the sintered porous sample and provide a comprehensive information on the porosity also in the 3D space, mentioned computed tomography (CT) technique was also used.

3. 3D tomography investigation

The computed tomography is an efficient technique providing a possibility for a 3D nondestructive investigation of a wide range of materials and their microstructure morphologies. It was also successfully used to investigate metallic materials, see e.g. [16,17]. Unfortunately, due to density of metals usually, very high-energy X-rays (generated e.g. by the synchrotron radiation) are required, limiting research capabilities. Fortunately due to the significantly different properties of a porosity and matrix this is not the case here.

Thus, in the present work the CT technique was performed with the use of the widely available laboratory scale equipment the Phoenix v|tome|x Industrial High-Resolution CT & X-Ray System providing 3D data on a microstructure morphology. The technique is based on a series of X-ray measurements realized on a rotating sample under different angles. As a result, a set of two-dimensional data on microstructure morphology at various cross-sections is obtained and further postprocessed by a computer 3D data reconstruction algorithms. Eventually, the 3D information on a microstructure morphology can be obtained in a non-destructive way. Unfortunately, quality of reconstruction directly depends on the data processing steps, what may often lead to significant inaccuracies in the 3D description.

The data obtained from the CT are usually stored in a binary format, which requires an additional metadata in order to import and further investigate them during postprocessing. In the current work the recorded CT binary data was stored in the. vol file, while the metadata was stored in the. vgi file, which contains information such as: data size, data type, data range or resolution. Although commercial software allows to visualize these kind of data and perform some general analysis, they are not designed to generate an input data for further numerical simulations based on the Digital Material Representation concept. To provide such capabilities and to convert data from the CT directly into the format compatible with a mesh generating software, the inhouse computer program was developed. It utilities series of steps:

- Preparation of data structures for a given type of metadata from a CT;
- Importing data and converting them into a 2D array of values representing a single section of an investigated sample. In this form obtained data are impossible to be properly assessed as seen in Fig. 7 and require additional processing operations;
- Mapping obtained values into 0–255 range and converting them into a grayscale image for memory efficiency (Fig. 8a);
- Performing an image thresholding where the first group of pixels represents a matrix material while the second a porosity (Fig. 8b);
- Stacking preprocessed 2D sections into the 3D array to obtain a complete volumetric information (Fig. 9);
- Exporting such volumetric data into the format compatible with the finite element mesh generation software.

The developed algorithm was implemented with the Python 2.7 programming language accompanied by a set of scientific libraries, such as the NumPy and SciPy. These programming toolkits have been selected as they offer large collection of algorithms and utilities dedicated for an advanced image processing operations as well as a numerical and a statistical analysis [18].

Again, like in the classical 2D investigation, the most important step in the developed algorithm was binarization operation. This step appeared to be crucial to extract the meaningful data regarding the sample and its morphological features from the initial CT 2D data sets. Unfortunately, the binarization procedure can have a direct impact on obtained morphology, also affecting the calculated porosity volume fraction. The Otsu thresholding method [19] was used to obtain the proper binary representation of the investigated data. The main advantage of the algorithm, is that it allows for an automatic calculation of the thresholding value based on a histogram of grey level input data from a set of CT scans (Fig. 10a). This step, however, cannot be performed without a supervision, as inaccurate identification of the thresholding value can lead to erroneous interpretation of the CT data. That is why the Otsu algorithm was additionally extended in the present work with the offset mechanism that allows manual modification of calculated thresholding value. Furthermore, to improve the data processing (e.g. remove artefacts in the form of a single-pixel pores or other disruptions) a dilation and an erosion operations were implemented. The image processing chain is presented in Fig. 10b.

Table 1 and Fig. 11 illustrate the significant impact of the thresholding value during a binarization operation on the obtained volume fraction of porosity in the CT scanned samples.

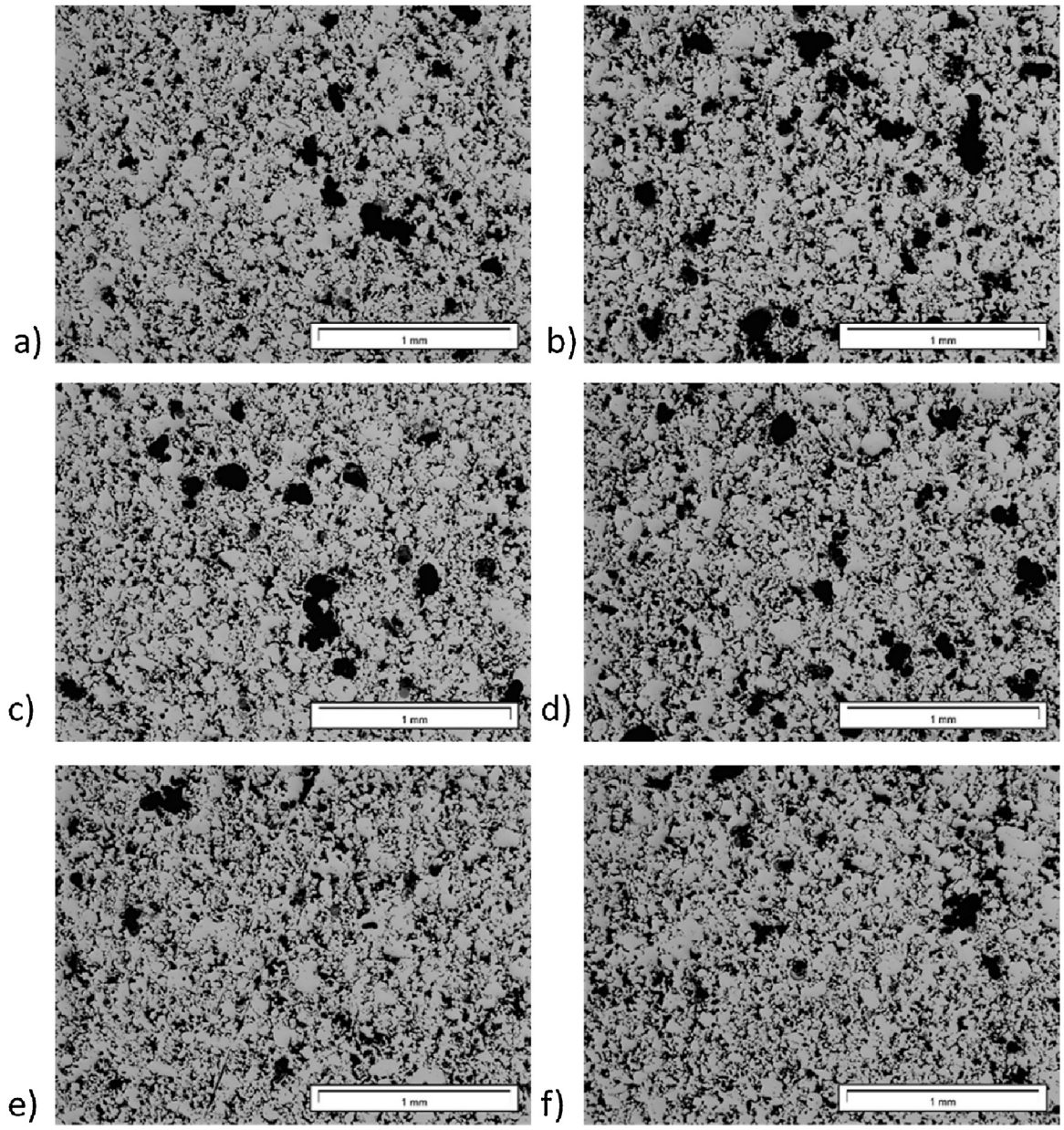

Fig. 5 – Examples of images obtained during the systematic scanning according the matrix from Fig. 4, (a) 2B, (b) 2C, (c) 3B, (d) 3C, (e) 4B, (f) 4C.

As seen in Table 1, even a small change in the thresholding value results in a significant change in the porosity fraction after the binarization. It can also be observed that when the threshold is set above the value calculated by the Otsu algorithm, a volume fraction increases but the number of pores drastically drops as they tend to merge into the bigger complex structures. To properly perform these operations and obtain reliable 3D data, an information on the porosity volume fraction evaluated with the different technique is invaluable. As mentioned, in the present work the hydrostatic weighting procedure was used to identify the proper thresholding level. Thus, the thresholding value for investigated volume was set as 169 to obtain approx. 25% porosity in the matrix material as illustrated in Fig. 12.

Additionally, to clearly identify subsequent pores in the investigated matrix the coloring algorithm was implemented and obtained results are shown in Fig. 13. Therefore, a statistical analysis of subsequent pores (e.g. volume distribu-

Table 1 – The relation between the threshold value and obtained volume fraction as well as the number of pores.

Threshold value	Volume fraction	Number of pores
152	4.92%	54
162	13.58%	129
167	21.1%	97
172 (calculated by Otsu)	31.75%	54
182	60.1%	14

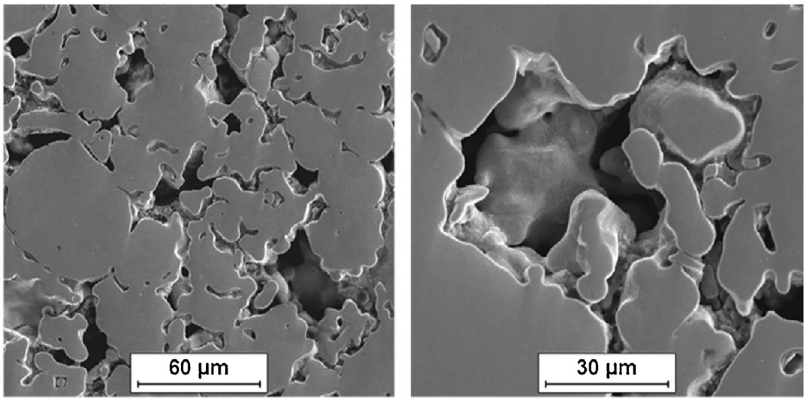

Fig. 6 – Examples of scanning electron microscopy images of sintered microstructure obtained with two different magnifications.

tion, geometrical parameters, dispersion, etc.) could be easily evaluated.

As presented, the CT technique provides significantly broader view on the 3D state of the microstructure morphology than 2D images. In the case of sophisticated 3D morphologies a two dimensional analysis can often lead to inaccurate results and conclusions. However, at the same time interpretation of obtained 3D data is much more complicated than the 2D ones. Also, the laboratory scale CT equipment has limitations in the energy sources and cannot distinguish smaller details of the microstructure morphology. In the present case study, the obtained CT data resolution provided a capability to accurately reconstruct pores with approx. 20 μm in the diameter. Thus, to perform a through scale investigation of the porosity with resolution better than the one obtained with the CT, another complementary technique was used during the research, namely the serial sectioning.

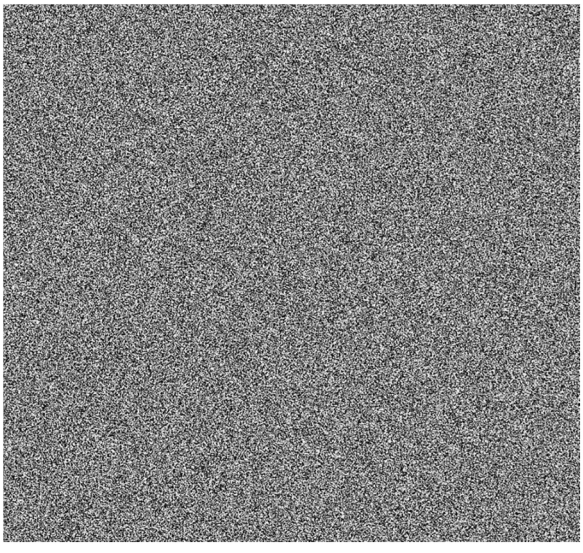

Fig. 7 – An example of raw data at a particular cross section directly obtained from CT measurements.

4. The 3D serial sectioning investigation

The serial sectioning procedure is not often used, as it is usually based on a time consuming and very precise manual labour. An automated serial sectioning can be realized with the use of specially designed equipment e.g. the RoboMet or the focused ion beam (FIB) tomography within the scanning electron microscope (SEM) chamber. In the former case, an access to such equipment and in the latter case, a small surface area that can be investigated are limiting factors.

In the present work a manual serial sectioning procedure has been performed to obtain a detailed high spatial resolution data. The sample was vibro-polished with the same procedure as presented in Section 2. To fix the imaging region for subsequent layers a set of deep indicators in the form of Vickers microhardness indents was introduced. Vickers indents were not only clearly visible under the microscope they were also used to evaluate the layer thickness h removed during a single polishing step, according to:

$$h = \frac{d_1 - d_2}{2 \cdot tg68^\circ} \tag{1}$$

where d_1, d_2 – diagonals of the indent prior and after polishing step, respectively.

In order to even capture the geometry of small pores (dimensions between 1 and 2 μm), the polishing setup was adjusted during the serial sectioning to remove 0.5 μm thick layer of the material. Thus, after a set of case studies, the 610 g vibro-polishing load and 12 min polishing time were applied. With these adjustments the required resolution, to represent a geometry of the smallest features by at least two to three 2D sections, was obtained. The polishing time was then additionally reduced to increase the sectioning resolution to approx. 0.15 μm. The overall depth of the removed material was 15 μm with the covered surface area of 132 μm × 132 μm.

After the each polishing step a high resolution image of the surface was recorded with the digital camera. As an outcome a set of 40 images of microstructure morphology from subsequent depths was obtained and subjected to image processing. The procedure to obtain a binary representation was the same

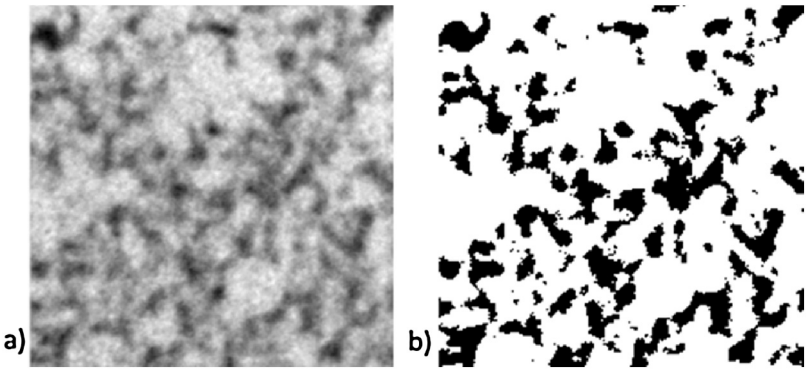

Fig. 8 – An example of visualization of the data for a single microstructure cross-section (a) in the grey scale mode and (b) in the binary mode.

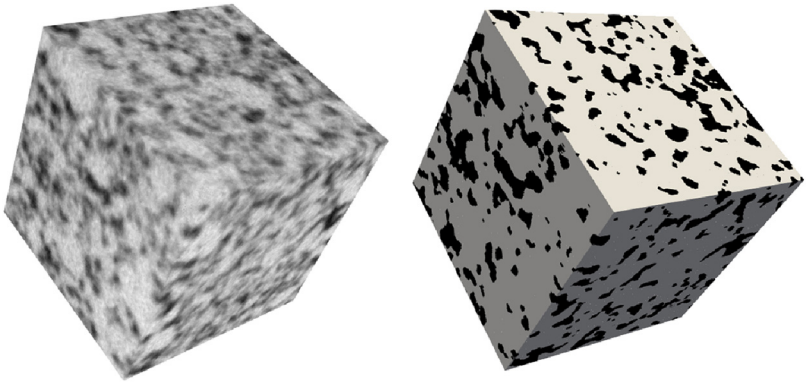

Fig. 9 – An example of visualization of the 3D volume of microstructure (a) in the grey scale mode and (b) in the binary mode.

as in Section 2. It has to be noted that subsequent images have to be precisely adjusted with respect to each other to avoid any artificial features or mismatch between the two sections. Images were translated and rotated manually to compensate the image acquisition uncertainties. This is crucial, as any misalignment directly affects the 3D reconstruction results. As mentioned, such an approach is highly time consuming and requires a high level of accuracy. However, it provides a

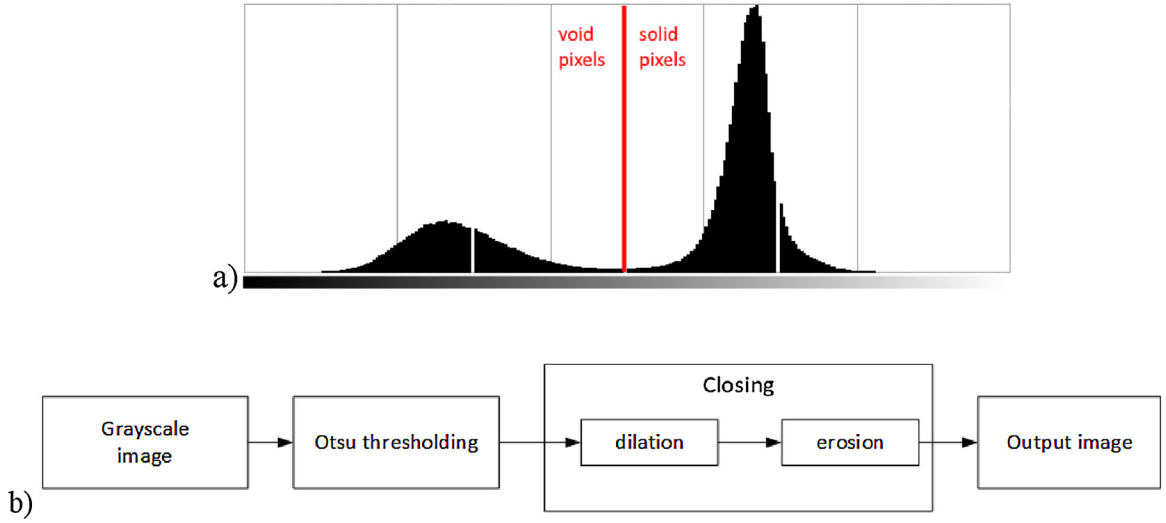

Fig. 10 – An illustration of (a) a histogram of grayscale image with peaks associated with matrix and porosity grey scale levels, (b) implemented image processing chain.

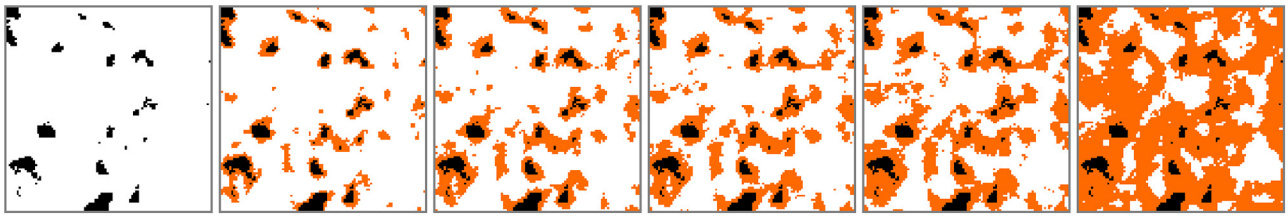

Fig. 11 – A cross-section of reconstructed samples using a set of threshold values: 152, 162, 167, 169, 172 and 182.

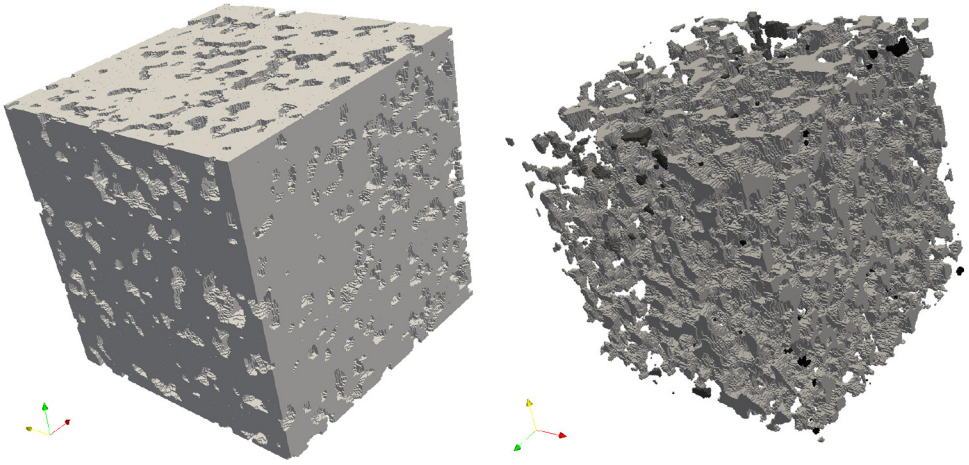

Fig. 12 – The digital model of (a) matrix (grey voxels correspond to the matrix), and (b) porosity obtained from the CT data (grey voxels correspond to the pores).

possibility to investigate porosities of dimensions within the range of 1 μm to approx. 15–20 μm. Thus, this technique perfectly complements the CT investigation.

Obtained 2D binary images of the porous microstructure morphology with clearly visible features representing pores at

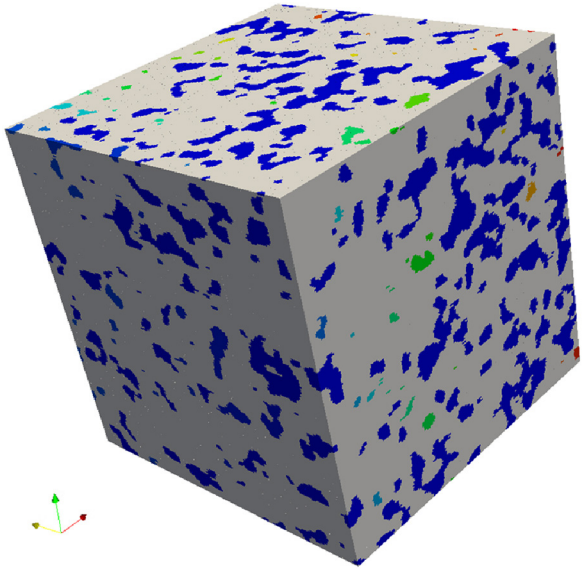

Fig. 13 – Digital model of the subsequent identified pores in the CT data.

cross sections were then used as an input for the developed 3D reconstruction algorithm. Reconstruction of a set of 2D sections to recover complete 3D information is critical for development of the digital material representation model for further finite element calculations. 3D FE models require a continuous, spatial volumetric data. The 3D reconstruction algorithm is based on an initial concept presented in [20], but significantly modified to improve the quality of volumetric results. Details of the proposed modifications and extensions are presented in the following part of the chapter.

The developed reconstruction algorithm is based on the three main steps, which can be summarised as follows:

1. *An automatic identification of matching pores in subsequent images* (Fig. 14). This is the crucial step that directly influences the quality of reconstruction.

The matching algorithm is based on the scanline flood fill (SFF) approach as described in [21]. In case of a 2D data the SFF algorithm investigates pixels from subsequent images line by line identifying cells in the same locations in the investigated spaces as illustrated in Fig. 15. To minimise the computational time specific data structures for already evaluated cells were developed, what reduces the amount of allocated memory and minimises time loses related to the recurrent execution of the algorithm. With this, the algorithm could be applied to large set of input data.

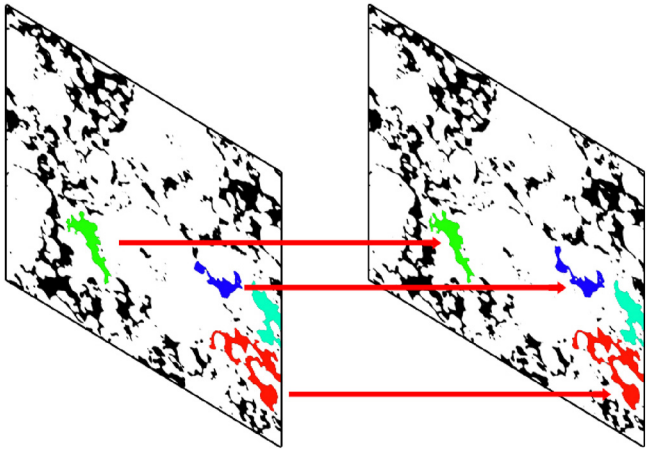

Fig. 14 – Automatic identification procedure of matching pores on two subsequent images.

The concept of the SFF algorithm was then extended in the present work to deal with the 3D computational domains. In this case the scan line was substituted by a plane as seen in Fig. 16.

It should also be noticed that the image processing operations were performed independently on each input microstructure photograph, what sometimes may result in an insufficient binarization with the automatic thresholding or small variations between sections after the application of post processing operations (e.g. dilatation/erosion). As a result, pores can be artificially removed from the processing image what is schematically presented in Fig. 17.

Such loss of information leads to an inaccurate reconstruction. From the algorithmic point of view during the pore matching operation the feature from section no. 1 will get different identification number than the feature from section no. 4. As a result artificial pores would be introduced into the reconstruction affecting the final 3D data. To correct such obvious discrepancies the matching algorithm has been extended to evaluate not only pair of images at the same time but to investigate series of them. In the developed solution, whenever the matching algorithm encounters a pore without continuation at the neighbouring section, it automatically extends the search procedure to the subsequent 2D sections. If the matching pore exists in one of the additionally evaluated sections, the algorithm performs correction of intermediate 2D sections and adds missing pores using an extraction procedure. In this case the overlapping area of matching pores is extracted to the intermediate sections. Eventually, matching and recovered pores from subsequent images are identified and marked with the same identification number as presented in Fig. 18.

2. *The 3D reconstruction of matching pores on subsequent images*. The algorithm operates in an iterative manner considering a pair of neighbouring images at a time. Due to the variations in the amount of removed material during the vibro-polishing between subsequent sections their spatial distribution is not constant. The reconstruction is performed in the computational domain with the physical dimensions, thus it is assumed that the number of reconstructed sections between two investigated images also varies. The developed algorithm before the data extrusion/interpolation automatically evaluates the distance and adjust number of additional sections. Therefore, the complete volumetric data can be reconstructed. The reconstruction algorithm evaluates the overlapping area of each pore from the two investigated sections and performs the extrusion procedure as seen in Fig. 19. The remaining non-overlapping areas of investigated pores are then reconstructed by the interpolation method as seen in Fig. 20.
3. *The automatic refinement of reconstructed pore shapes*. During the interpolation stage some of the pore edges may become highly irregular. This is a non-physical artefact. In order to smoothen the edges a grain growth algorithm based on the Monte Carlo method [8] was implemented. To maintain the geometry of reconstructed porosity as close as possible to raw input data only a single step of the MC algorithm is applied. Examples of the MC processed shape of a single pore are presented in Fig. 21.

All remaining single cell artefacts are then evaluated to establish if they belong to the porosity or to the matrix material. The implemented denoising algorithm is based on the cellular automata method with the Moore neighbourhood definition [8]. As shown in Fig. 22, in the approach the investigated cell (blue) that has less than two neighbours (green) is eliminated from the image.

Presented three steps of the developed algorithm lead to the 3D reconstruction of a set of two dimensional input data as presented in Fig. 23.

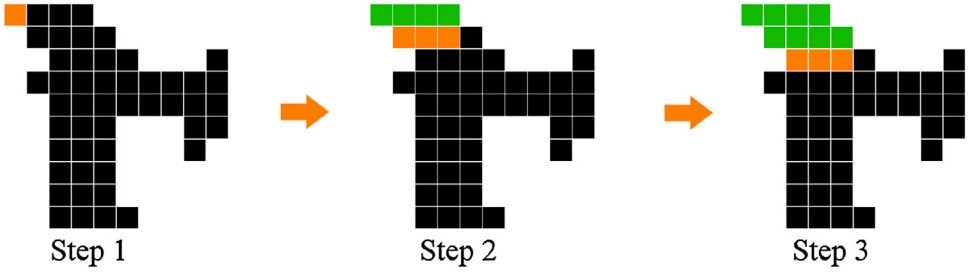

Fig. 15 – Visualization of subsequent steps of the scanline flood fill algorithm in a 2D space.

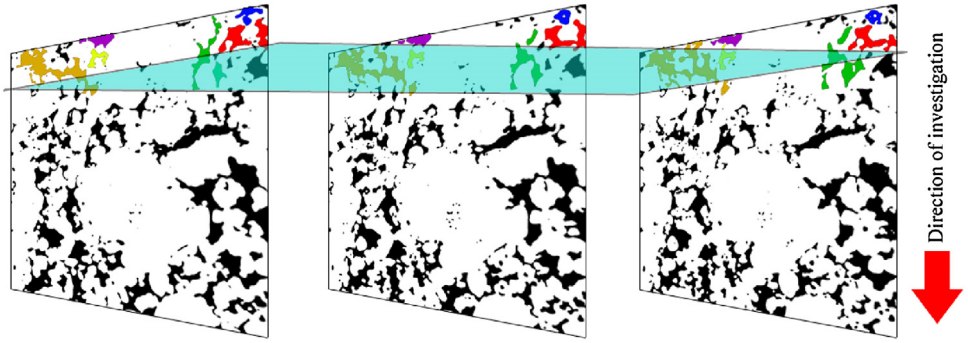

Fig. 16 – Concept of the scanline flood fill algorithm in a 3D.

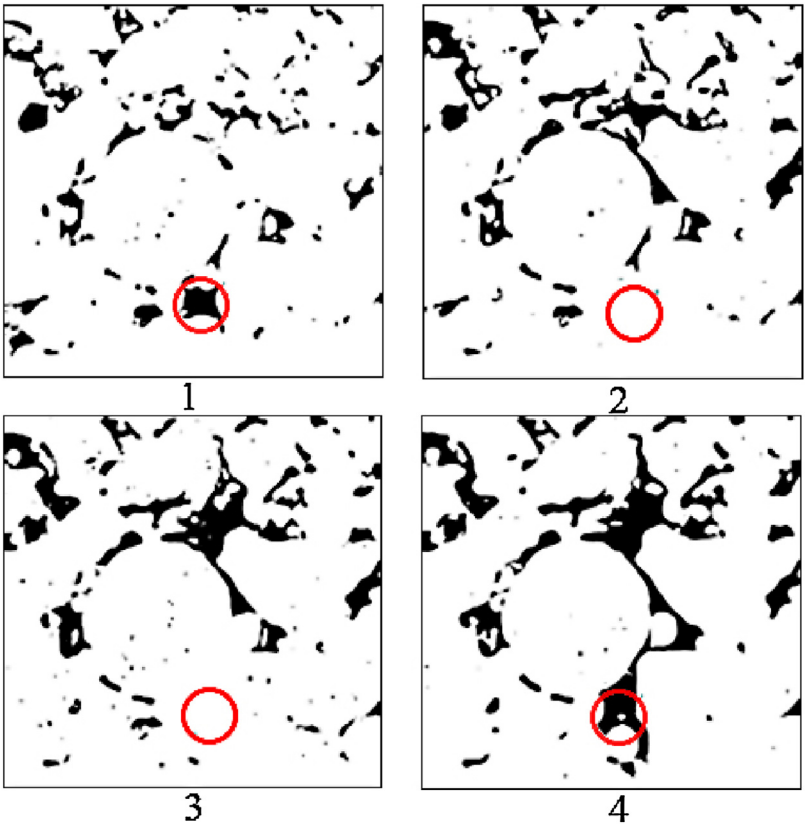

Fig. 17 – Illustration of a possible influence of the image processing on the morphology representation at subsequent sections.

The detailed representation of the porosity without the visible matrix is presented in Fig. 24.

The reconstructed 3D microstructure can be analysed directly in the 3D space in any direction. With each feature described by a different id number there is also a possibility to measure quantitative parameters of the structure e.g. the volume fraction of pores in the sample, the surface area, the volume of pores, the Feret diameters in different directions, etc. Additionally, the reverse analysis is possible: 3D reconstructed structure can be sectioned in a selected direction to obtain the 2D cross section. However, as was presented within the paper, application of only 2D investigation may result in misleading information on geometrical aspects of a porosity.

Information provided by the reconstructed 3D digital microstructure across various length scales regarding positions of pores within the material, obtained based on the combination of CT and SR, can be then an input for the finite

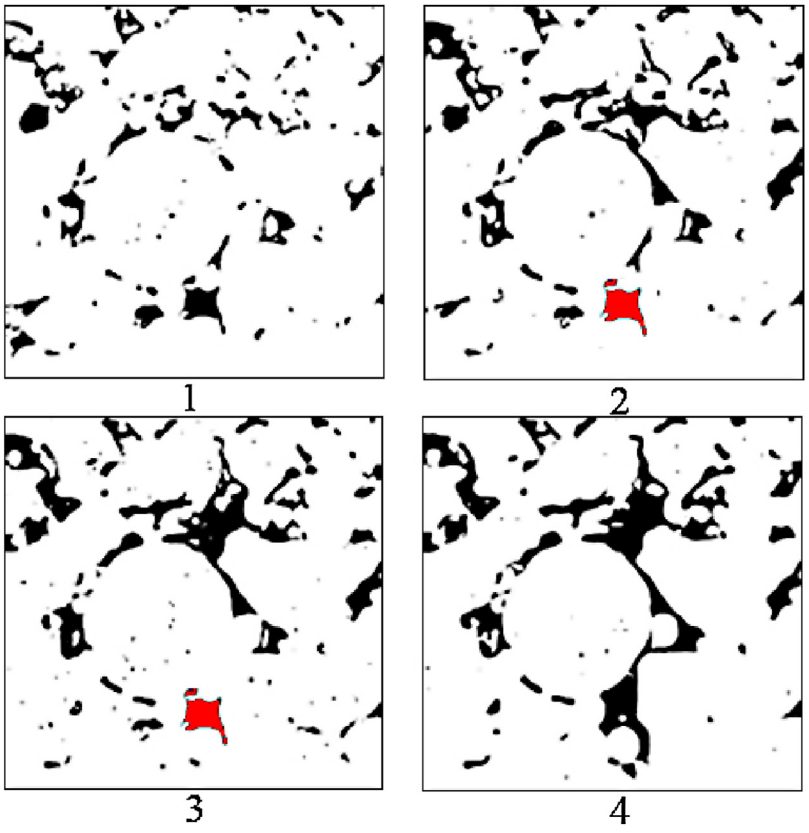

Fig. 18 – Example of pores on subsequent images identified by the developed matching algorithm.

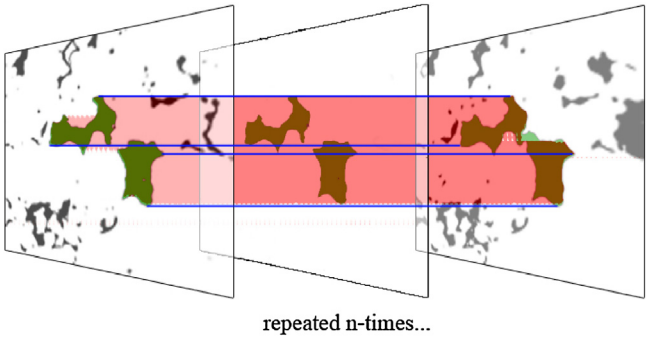

Fig. 19 – Concept of the extrusion of overlapping area of matching pores.

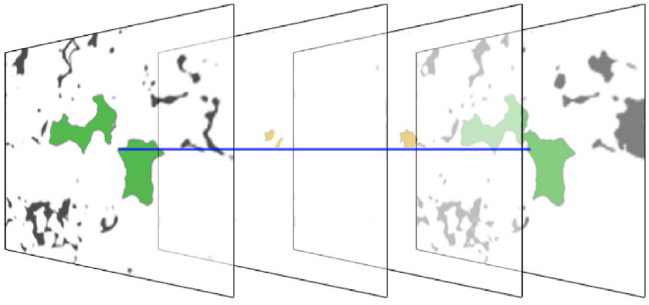

Fig. 20 – A concept of the reconstruction of a non-overlapping area of matching pores.

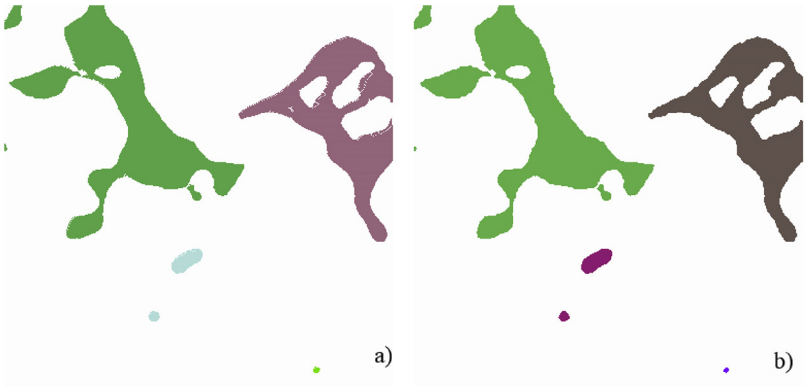

Fig. 21 – Pore edges (a) before and (b) after execution of the smoothing algorithm.

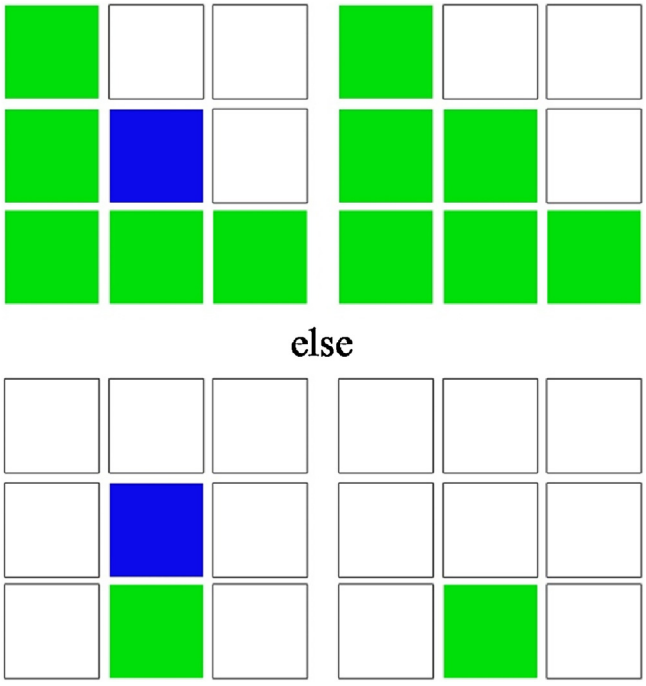

Fig. 22 – Illustration of the denoising algorithm.

element investigation of a sintered sample behaviour under loading conditions.

5. The digital material representation models based on experimental investigation

The numerical analysis with the digital material representation model generated based on the described CT data was selected as a case study within the paper. The exported reconstructed 3D morphological data were discretized with the finite element mesh and incorporated into the commercial Abaqus software. The 3D tetrahedral mesh was generated across the computational domain with the in-house DMRmesh software [22]. Additionally, to capture the complex morphology of sintered porous microstructures the mesh was automatically refined along the porosity boundaries as seen in Fig. 25. The isotropic hardening material model was selected with the flow stress data of the solid matrix obtained from the set of local nano-indentation tests on the Hysitron TI 950 TriboIndenter. The measured load–displacement values have been recalculated to a stress–strain response with the use of the inverse analysis approach and then assigned to

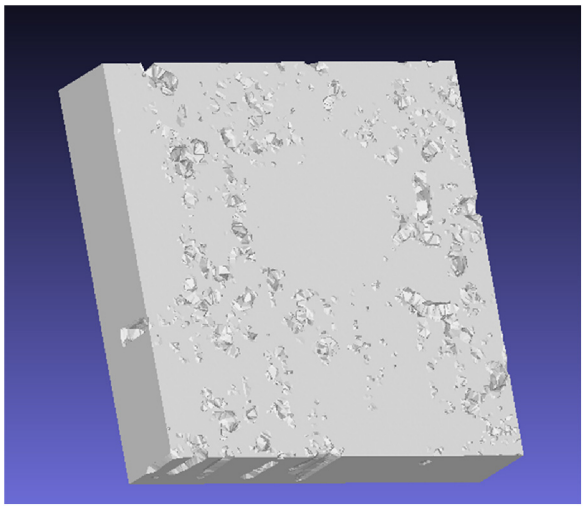

Fig. 23 – The reconstructed volume of the investigated porous microstructure from the serial sectioning operations.

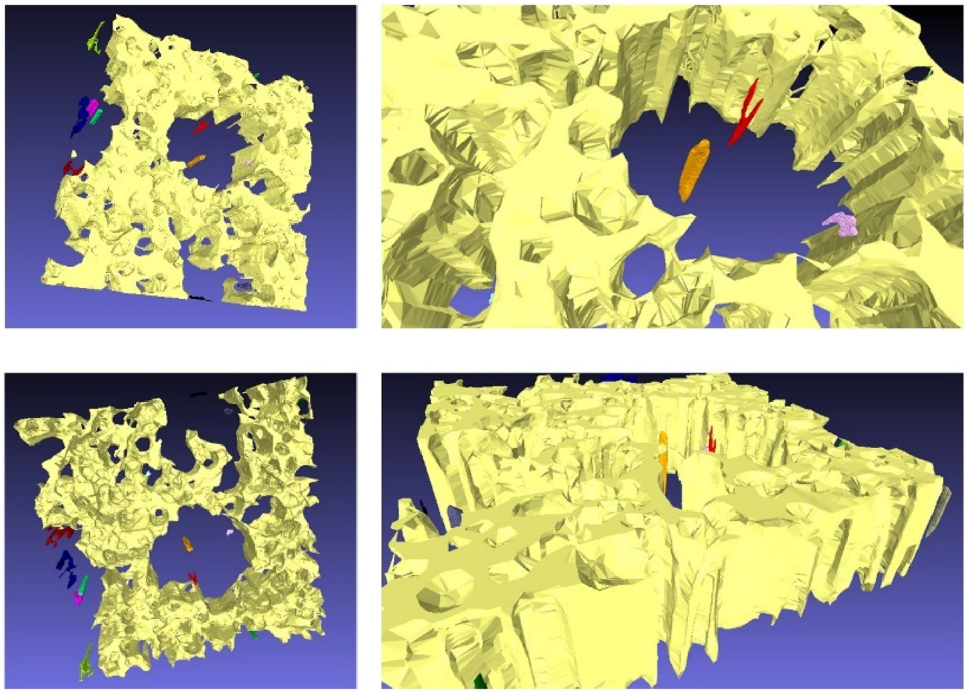

Fig. 24 – The reconstructed volume of the investigated porous microstructure from the serial sectioning operation with subsequent pores represented by different colours. The physical size of the sample is 132 μm × 132 μm × 15 μm.

the matrix material in the FE model. To present capabilities of such microstructure based modelling, a complex deformation conditions occurring during the compression with an additional torsion were replicated in the developed numerical model. Examples of results from the numerical model are presented in Fig. 26.

The numerical model of the sintered sample with an explicit representation of a porosity provides an insight into the material without an extensive experimental investigation. Changes in the pore geometry as well as their behaviour during compression can be exactly evaluated. Strain and stress field provide also valuable data on pore closing, during compression and during superimposed torsion. The joining process within the porosity can be investigated. All the above mentioned issues directly influence the material hardening behaviour that can be predicted without any model simplifications.

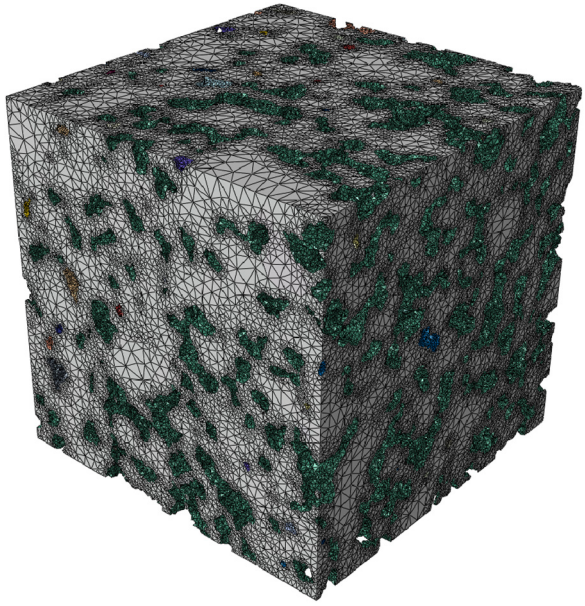

Fig. 25 – The DMR model of the investigated sintered material with the generated heterogenous finite elements mesh.

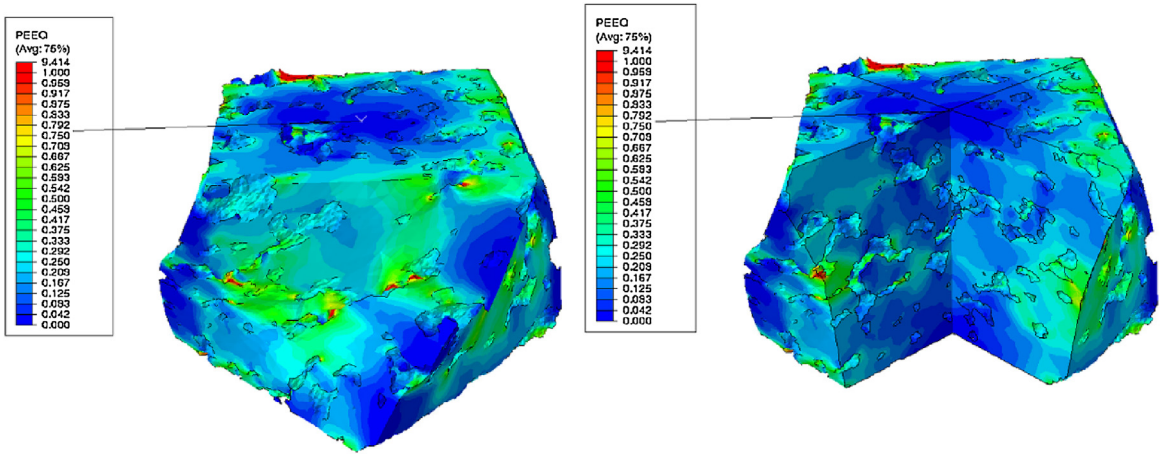

Fig. 26 – An example of local inhomogeneities in the strain field predicted by the digital material representation model generated from the CT data.

6. Conclusions

Based on the presented research the following conclusions can be drawn:

1. The 2D investigation of the porosity may yield misleading interpretations of the geometrical aspects of a microstructure morphology.
2. The extensive 2D systematic scanning investigation can provide statistically meaningful results regarding the porosity volume fraction.
3. The computer tomography can provide a complete 3D data set on the porous sample morphology, however it is highly sensitive to the image analysis setup, namely the selection of the threshold value.
4. The complementary porosity measurement technique should be applied to evaluate the appropriate thresholding value for the image analysis.
5. The high resolution manual serial sectioning provides a detailed 3D data even on the small pore sizes.
6. The combination of a serial sectioning and a computed tomography provides through scale investigation of the 3D morphology of sinters.
7. The 3D digital material representation model generated basing on the experimental investigation results provides detailed information of the pore behaviour under deformation conditions, even in case of the complex loading paths.

Funding body

National Science Center.

Acknowledgements

Financial assistance of the National Science Center project No. 2014/15/B/ST8/00086 is acknowledged. Numerical calculations have been performed with the use of the PLGrid Infrastructure.

REFERENCES

[1] X.P. Qin, L. Hua, Deformation and strengthening of sintered ferrous material, J. Mater. Process. Technol. 187–188 (2007) 694–697.
[2] N. Chawla, X. Deng, Microstructure and mechanical behavior of porous sintered steels, Mater. Sci. Eng. A 390 (2005) 98–112.
[3] J. Segurado, E. Parteder, A.F. Plankensteiner, H.J. Böhm, Micromechanical studies of the densification of porous molybdenum, Mater. Sci. Eng. A 333 (2002) 270–278.
[4] N. Bilger, F. Auslender, M. Bornert, J.-C. Michel, H. Moulinec, P. Suquet, A. Zaoui, Effect of a nonuniform distribution of voids on the plastic response of voided materials: a computational and statistical analysis, Int. J. Solids Struct. 42 (2005) 517–538.
[5] C. Soyarslan, C. Bargmann, M. Pradas, J. Weissmüller, 3D stochastic bicontinuous microstructures: generation, topology and elasticity, Acta Mater. 149 (2018) 326–340.
[6] F. Fritzen, S. Forest, T. Böhkle, D. Kondo, T. Kanit, Computational homogenization of elasto-plastic porous metals, Int. J. Plast. 29 (2012) 102–119.
[7] S. Bargmann, B. Klusemann, J. Markmann, J.E. Schnabel, K. Schneider, C. Soyarslan, J. Wilmers, Generation of 3D representative volume elements for heterogeneous materials: a review, Prog. Mater Sci. (2018), http://dx.doi.org/10.1016/j.pmatsci.2018.02.
[8] L. Madej, Digital/virtual microstructures in application to metals engineering – a review, Arch. Civil Mech. Eng. 17 (2017) 839–854.
[9] L. Rauch, L. Madej, Application of the automatic image processing in modelling of the deformation mechanisms based on the digital representation of microstructure, Int. J. Multiscale Comput. Eng. 8 (2010) 343–356.
[10] W. Kayser, A. Bezold, C. Broeckmann, EBSD-based FEM simulation of residual stresses in a WC6wt.-%Co hardmetal, Int. J. Refract. Met. Hard Mater. 73 (2018) 139–145.
[11] Y. Hou, T. Sapanathan, A. Dumon, P. Culiere, M. Rachik, A novel artificial dual-phase microstructure generator based on topology optimization, Comput. Mater. Sci. 123 (2016) 188–200.
[12] G.J. Schmitz, U. Prahl, Handbook of Software Solutions for ICME, Wiley-VCH, 2016.
[13] L. Wojnar, K.J. Kurzydlowski, J. Szala, Quantitative image analysis, ASM Handbook Metallography and Microstructures, vol. 9, 2004, pp. 403–427.
[14] J. Szala, J. Cwajna, A. Wisniewski, The systematic scanning and variance analysis method for the evaluation of particles distribution, Acta Stereol. 8 (2) (1989) 237–242.
[15] J. Chraponski, M. Malinski, J. Szala, J. Cwajna, FGM structure characterization by distance functions and systematic scanning method, Mater. Sci. Forum 567–568 (2007) 153–156.
[16] G. Nicoletto, G. Anzoletti, R. Konecna, X-ray computed tomography vs. metallography for Pore sizing and fatigue of cast al-alloys, Procedia Eng. 2 (2010) 547–554.
[17] A. du Plessis, P. Rossouw, X-ray computed tomography of a titanium aerospace investment casting, Case Stud. Nondestruct. Test. Eval. 3 (2015) 21–26.
[18] M. Blackledge, D. Collins, D. Koh, M. Leach, Rapid development of image analysis research tools: bridging the gap between researcher and clinician with pyOsiriX, Comput. Biol. Med. 69 (2016) 203–212.
[19] N. Otsu, A threshold selection method from gray-level histograms, IEEE Trans. Syst. Man, Cybern. 9 (1979) 62–66.
[20] L. Madej, M. Mojzeszo, J. Chraponski, S. Roskosz, J. Cwajna, Digital material representation model of porous microstructure based on 3D reconstruction algorithm, Arch. Metall. Mater. 62 (2017) 563–569.
[21] C. Bond, An Efficient and Versatile Flood Fill Algorithm for Raster Scan Displays, Notes from www.crbond.com2011.
[22] M. Madej, F. Kruzel, P. Cybulka, K. Perzynski, K. Banas, Generation of dedicated finite element meshes for multiscale applications with delaunay triangulation and adaptive finite element – cellular automata algorithms, Comput. Methods Mater. Sci. 12 (2012) 85–96.